Image-driven model building for ray-tomography: increasing confidence in exploring the MSGBC Basin (NW-Africa)

Paolo Esestime[1], Zhiqiang Guo[1], Li Li[1], David Went[1*], Felicia Winter[1] and Ben Sayers[1] present a seismic tomography method applied to the processing of 28,000 km² of seismic data in depth, which included multiple 3D seismic campaigns from 2011 to 2019.

Introduction

Seismic tomography is an inversion-based technique, long-established as industry standard and routinely performed to obtain velocity models for depth migration. Modern data and high-end computing allow performing tomography on extensive 3D seismic data, acquired in frontier as well as mature basins. We present an example of the method applied to the processing of approximately 28,000 km^2 of seismic data in depth, which included multiple 3D seismic campaigns from 2011 to 2019.

TGS, in partnership with PGS and GeoPartners, simultaneously processed all those data through a common sequence, and created a new 3D multi-client dataset: the JAAN 3D, meaning the snake in Wolof Language (Figure 1).

JAAN 3D extends over a prospective offshore basin, largely underexplored, crossing the countries from Senegal to Guinea-Bissau, in water depths ranging from 100 to 3000 m. TGS data in the MSGBC region allows geologists to develop an unprecedented regional picture of the offshore continental shelf to derisk further exploration and repeat the success obtained with the oil and gas discoveries of Sangomar-1 (well SNE-1) and the discovery well Fan-1 (Figures 1 and 2). The depth imaging workflow is based on layered tomography, which updates velocity in a top-down sequence. Geological models and interpretations are integrated into the tomography for an optimal estimate of the fine-tuned velocity models. We use seismic moveout and available geological information to build the best possible pre-SDM anisotropic depth velocity model. The model is evaluated by the flatness of pre-SDM gathers, clarity of pre-SDM images and well misties if applicable. Well information is lacking in this region for the depth-imaging workflow. The regional structural and stratigraphic framework was calibrated and interpreted from the underlying TGS 2D seismic data grid, a modern dataset acquired between 2012 and 2017, which ties relevant seismic events and discoveries.

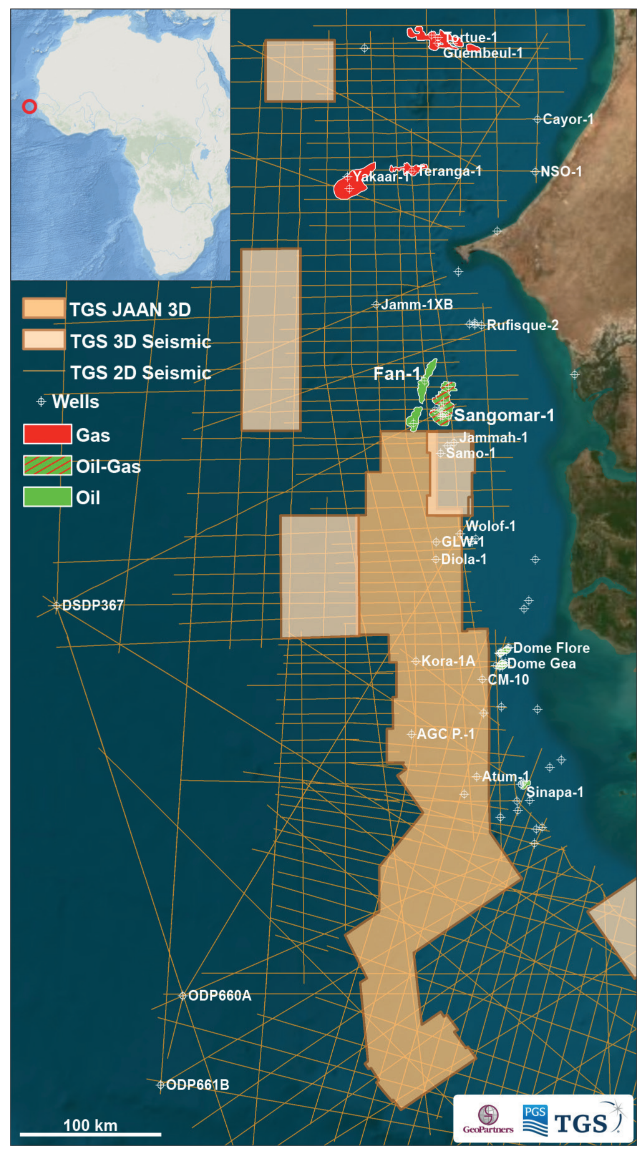

Figure 1 Map of the TGS multi-client seismic library in the MSGBC Basin showing relevant wells and hydrocarbon discoveries.

Exploration targets and imaging challenges

The MSGBC is a collection of offshore basins and is an acronym of the countries onshore, namely Mauritania, Senegal, Gambia, Guinea-Bissau and Guinea-Conakry. The basin has a common

[1] TGS
[*] Corresponding author, E-mail: David.Went@tgs.com
DOI: 10.3997/1365-2397.fb2020040

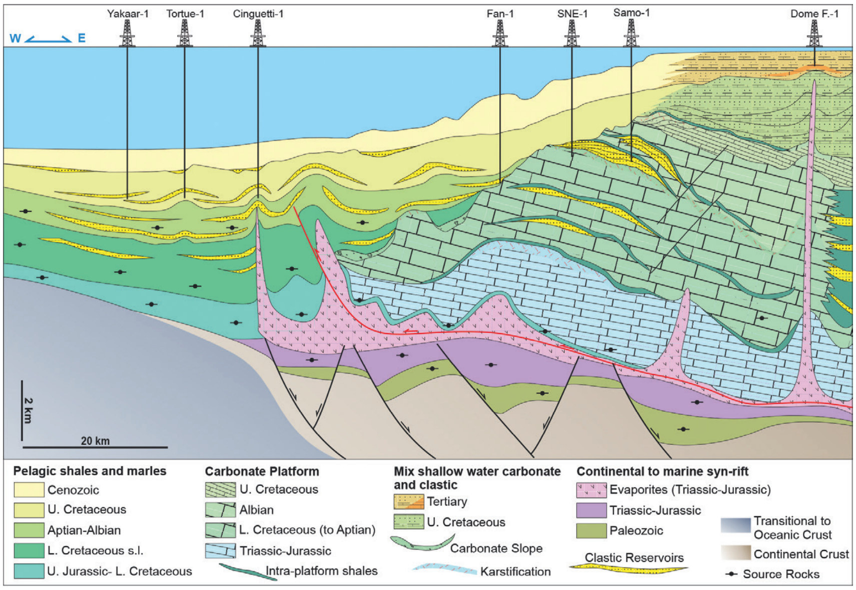

Figure 2 Schematic geo-seismic section including the regional sequences, the hydrocarbon plays and the exploration targets. The section is focused on the MSGBC Basin area which is covered by the JAAN 3D seismic survey.

tectonic and sedimentary evolution commencing with the deposition of carbonates and siliciclastics in a Palaeozoic-Triassic rift, followed by local oceanization as early as the Late Jurassic period (Davison, 2005). The marine transgression is mainly Jurassic and is associated with deposition of shallow water carbonates and evaporites (Soto et al., 2017). The carbonate platform persisted regionally on the continental margin during the Cretaceous period. It includes some siliciclastic intercalations in later times. Meanwhile, the abyssal plain records a continuous deposition of interbedded shales and sands (Figure 2).

The crustal stretching mainly pre-dates the Atlantic rifting, but the effect of passive thermal subsidence is clearer from the Early Cretaceous period. From this time, the MSGBC basin finally became part of the Atlantic margin of north-west Africa. Localized Late Cretaceous compression and salt movements are the main causes of deformation and the development of structural traps in both carbonate and clastic reservoirs. The platform was eventually detached at the evaporite level, with consequent folding and buttressing of the pelagic layers along the slope (Figure 2). Tectonic and salt structures are common along the shelf, along with associated phases of uplift, with erosion and karstification of the carbonate platform and formation of reefs and build-ups along its margins.

Continental to marine source rocks are present in the Upper Jurassic to Lower Cretaceous syn-rift section, and potentially in intraplatform shales and marls. In deep and ultradeep water, organic-rich shales have been proven at multiple levels in the Jurassic, Aptian and Cenomanian (Brownfield, 2016). The depth imaging of the JAAN 3D facilitates the mapping of potential Jurassic to Lower Cretaceous source rocks beneath the carbonate shelf, which has, until now, been notoriously difficult. These deep units in the basin can be correlated with the early stage of growth of the platform domain. In sectors characterized by minimal deformation JAAN 3D shows a clear onset of the early platform on to existing clastic deposits which are laterally continuous to basinward pelagic units. Potential source rocks associated with this interval can be traced laterally beneath the carbonate platform (Figure 3). The future integration of geochemical data with seismic mapping is needed to develop a more comprehensive model correlating source rocks, migration and charge of hydrocarbon (Sayers and Cooke, 2018).

The carbonate slope is a key factor linking hydrocarbon migration and charge from pelagic source rocks to clastic and carbonate reservoirs. Hydrocarbon accumulations are proven in sand reservoirs onlapping the carbonate slope (well Fan-1, Figure 1). The number and size of structural-stratigraphic closures present at

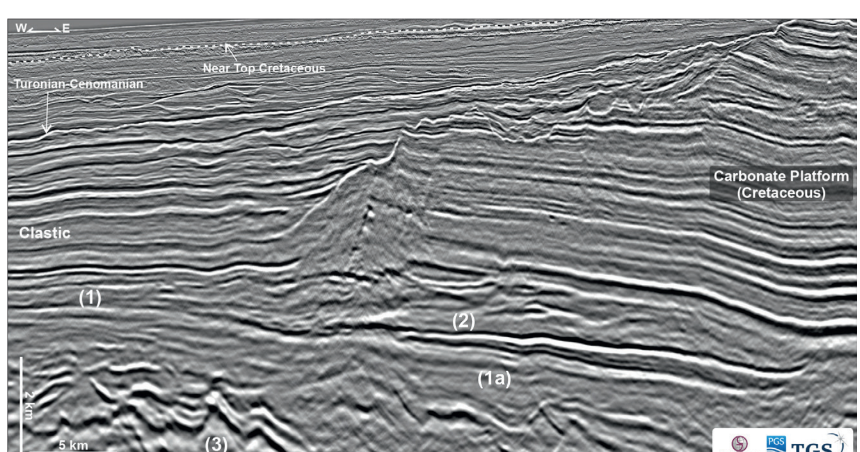

Figure 3 Kirchhoff Pre-SDM section extracted from JAAN 3D. (1) and (1a) Triassic-Jurassic or younger shales, potentially organic-rich; (2) Platform paleo-shelf; (3) Evaporites and continental to marine clastic syn-rift. The deep continuous events marked in (1) and (1a) suggest that source rocks may extend deep beneath the carbonate platform.

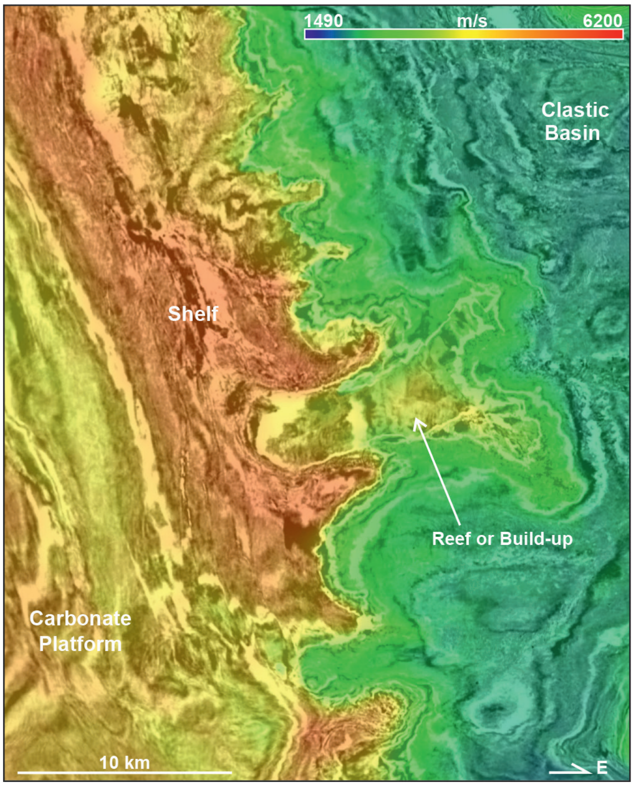

Figure 4 Final depth interval velocities overlain on a Kirchhoff Pre-SDM depth slice. The slice shows a good geological consistency between horizons and velocity field along the carbonate shelf, and the contact between carbonate and clastic.

the platform to basin transition suggest that future discoveries are to be expected in this area. JAAN 3D strategically 'snakes' across the highly prospective Cretaceous shelf.

The tomography workflow was set to model the seismic velocities accounting for the greater variability across the transitional area. Several interim steps of migrations (Kirchhoff) are used to test the amplitude recovery, and to obtain a velocity field geologically consistent with seismic events and changes in lithofacies, such as carbonate build-ups, salt-related structures and at contacts between carbonates and clastics (Figure 4).

The recovery of the seismic energy from intraplatform events was a key objective for the imaging to recognize lateral changes in facies and diagenetic history, which impact the seal effectiveness and the reservoir quality, in both carbonates and clastics.

The depth imaging workflow was set to identify the anomalous velocities potentially present in the shallow water and within the platform areas. As a result, the amount of noise has been reduced, boosting the amplitudes of intracarbonate events and overcoming the limitations imposed by the time migration (Figure 5). Furthermore, to fully understand the trapping mechanism in the giant discoveries like Sangomar, depth imaging is critical for locating closures and accurately mapping hydrocarbon volumes.

In deep water, the internal architecture of clastic targets is the result of combined mass transport and seafloor currents, which form a mixed system of turbidites and contourites. Seismic mapping and post-stack attributes, such as amplitude envelopes, spectral decomposition and RMS amplitudes, suggest reservoirs may have complex connectivities, particularly in up-dip pinch out settings where tuning effects further complicate interpretation.

Prospect generation commonly requires AVO support. Velocities obtained from migration velocity analysis can be used to build a background low-frequency model for AVO inversions targeting the elastic and petrophysical properties. The velocity modelling was optimized to produce detailed velocity fields which exhibit geological conformity with complex statigraphy and small-scale structures in the deep-water sediments (Tiwary et al., 2020).

Tomography model-building workflow

A tomography model-building workflow is intended to incorporate geological information to refine the V_{int} (Interval Velocity) through tomographic updates (Figure 6). Seismic velocities are primarily defined as V_{rms} (root mean square velocities) for time migration. However, for depth migrations interval velocities are additionally required. The initial depth interval velocities can be converted from V_{rms} that derive from Pre-STM gathers (Al-Chalabi, 2014). This is followed by several iterations of tomographic updates to generate a stratigraphic model. The final velocity model is one that achieves an optimal flatness of Pre-SDM gathers and simultaneously follows the geometry of the geological bodies.

Geological constraints for the velocity model

Geological constraints can inform the velocity modelling by imposing the geometry and the values of the velocity field. A conditioned velocity model is then updated through tomography to reduce the RMO (Esestime et al., 2016). Layers and geobodies, with outlying velocities, can be inserted into the model if the

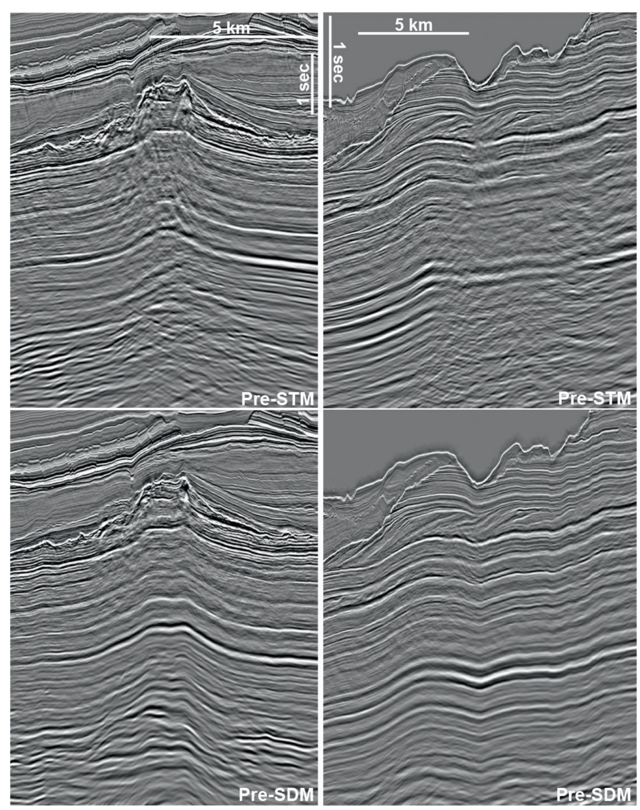

Figure 5 Pre-STM (above) vs Pre-SDM (below). Depth sections are stretched to TWT by using the final depth interval velocities obtained for depth migration. Improvements are visible within the carbonate shelf (bottom left) and the platform, where seafloor canyons are present (bottom right).

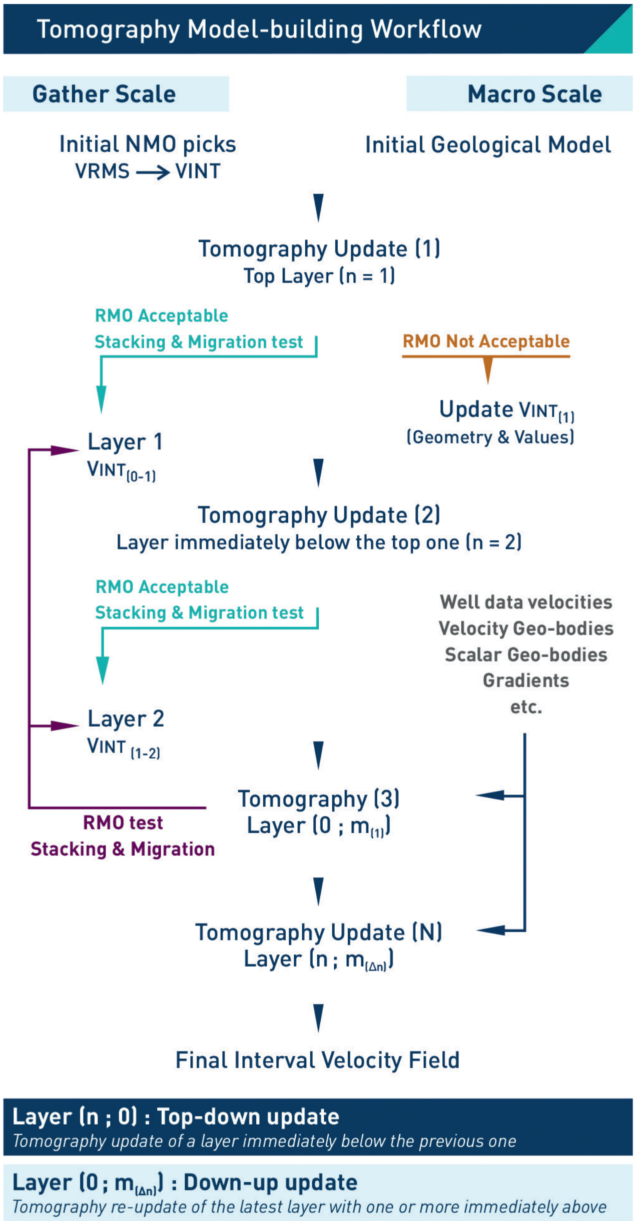

Figure 6 Generalised workflow of velocity modelling based on the image driven model building tomography. The layers are initially defined by a geological model. This model can subsequently be refined during several iterations and additionally be integrated with other data where available.

geologist and interpreters have a good understanding of the subsurface. These layers may show anomalous V_{int} and be due, for example, to salt or carbonates. These can be then identified in stacked sections as well as at the gather-scale and residual NMO correction made accordingly (Esestime et al., 2018). Eventually, velocity flood can be applied for defined geobodies. Interpreted horizons are made available from volumes at the early stage of processing to refine the V_{int} in both time and depth imaging exercises (Benson et al., 2015). The approach can be reiterated by updating the interpretation from interim stacks migrated after each step of tomography.

Geological constraints for tomography

Geological constraints can shape the reference geometry the tomography utilizes to ray-trace the energy and are sometimes referred to as "*tomographic meshes*". Guillaume et al. (2012) suggest that a layer-based mesh helps to stabilize the RMO in shorter and more homogeneous intervals consistent with velocity changes. The layers are progressively updated in a top-down sequence (Figure 6).

In JAAN 3D, the geological intervals and the imaging targets were already defined from the underlying 2D seismic data (Figure 1). A layered mesh was defined using the stratigraphic control provided by the horizon picks (Figure 7). Strong velocity changes were calculated at the contact between the carbonates and clastics and to a lesser extent at the regional unconformities (Figure 2).

Special attention is required for the top layers, as those control the stability of the following steps of tomography in the layer beneath. Water column velocities utilize sea-floor depth data so that the processing can be updated in sequence down to the first and the second interface. Thereafter, the results obtained from the tomography can be monitored using gamma plots (Figure 8) which can be extracted at any mesh boundary. A good approach is to extract gamma plots at defined targets or at secondary velocity interfaces and to use these to define additional meshes for the geological model.

As the shallow layers are gradually added and updated, the tomography extends to the deeper meshes. The stability of all intervals already updated can be tested by rerunning updates of the tomographic inversion (Bottom-up updates, Figure 6). Assuming the gamma plot and gathers show a clear improvement, the work can add one more depth layer to the model (update-iteration 4,

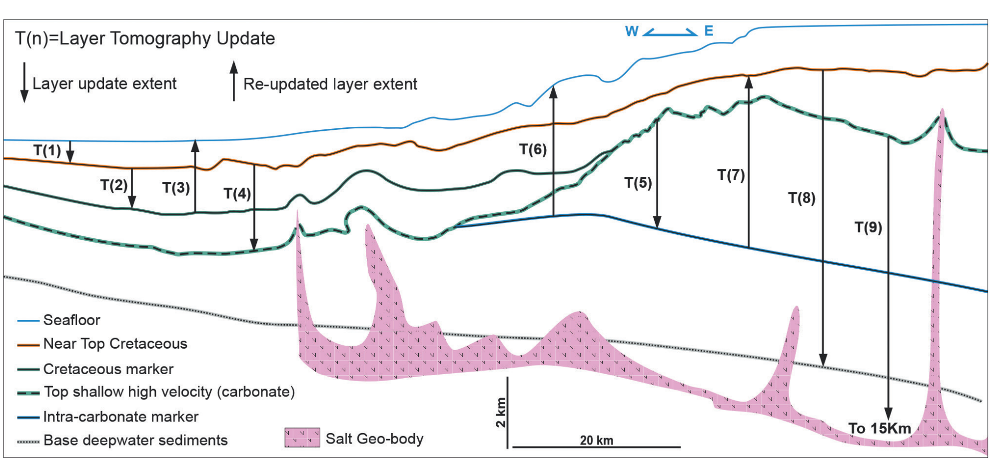

Figure 7 The schematic section summarizes the horizons and the geo-bodies in the geological model used to guide the depth imaging workflow. The layers identify the boundaries of the tomographic update. Downward arrows include layers updated for the first time and following a top-down sequence. Upward arrows include single or multiple layers updated as a test to stabilize the results obtained, known as 'down-up update'.

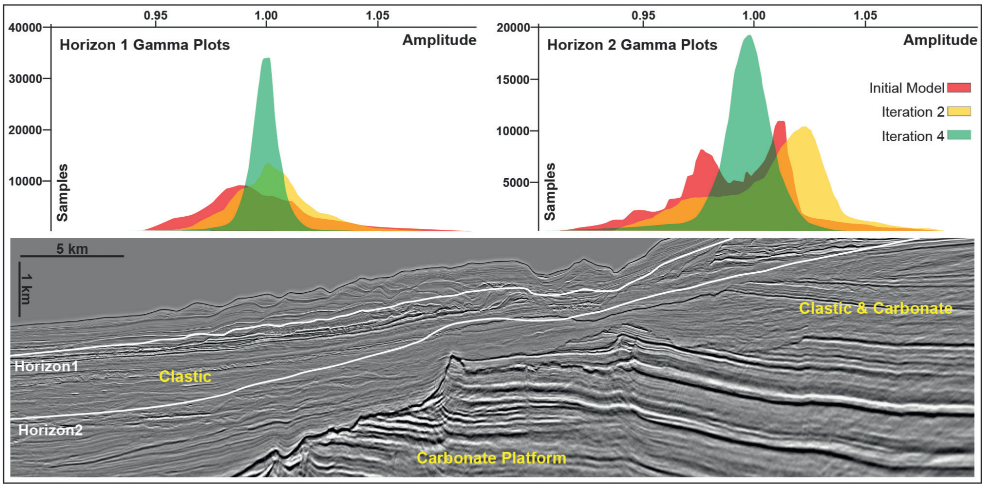

Figure 8 Gamma plots to statistically evaluate the amplitude recovered after every tomographic update. The amplitude values are extracted on relevant horizons and target events, from interim migrated volumes (Kirchhoff) obtained at each tomographic update.

Figures 7 and 8). Once a layer is stabilized, anisotropy parameters can be updated to further flatten the gathers. Since there is a lack of well data in this area, the initial anisotropy parameters delta and epsilon are built to be horizon-dependent and later updated through the model-building process. We plot the histogram of gamma to see the distribution of residual moveout. The ideal values for mean and standard deviation in the histogram are one (unity) and zero respectively. After several iterations of tomographic updates, mean values of gamma are close to 1, indicating that the residual moveout is greatly reduced. Updates of stable layers do not significantly change once the gamma plot shows a stable gaussian distribution, boosting the amplitudes and allowing the velocity field to match geological structures (Figure 9).

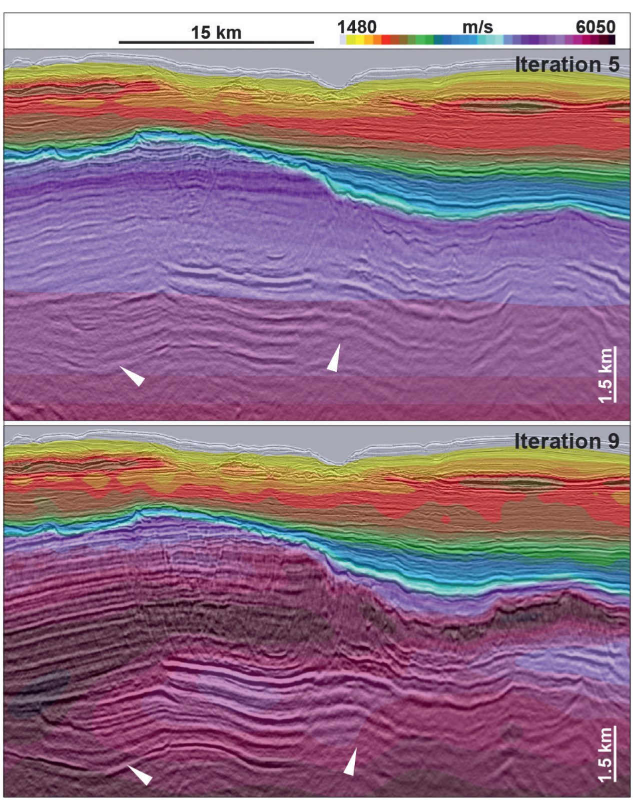

Figure 9 Interval velocity field overlain on the corresponding interim migrated amplitude stack (Kirchhoff). Clear improvements are visible in the amplitude response of iteration 9 (below) when compared to iteration 5 (above).

Conclusion

The inclusion of geological information into depth models allows tomography to derive velocity models more efficiently by reducing the number of processing iterations and results in a velocity model that conforms to the geological structure of the subsurface. It can be used in underexplored areas to accelerate the exploration process. Geological velocities from wells are not crucial, since the workflow is data driven. However, if well data is available it can be used to calibrate the velocities and estimate anisotropic parameters and for quality control at any stage of the workflow by checking depth mis-ties. The depth imaging on JAAN 3D demonstrates the workflow is applicable to extensive 3D volumes and allows for the joining together of areas with different geological settings and multiple imaging targets, including those with challenging carbonate and salt structures. The imaging workflow is based on amplitude recovery and the improvement of signal-to-noise ratio for stacking and depth migration algorithms. The velocity model is built and refined on the image quality uplift obtained through each tomographic update. The amplitude-friendly nature of this workflow ensures the final migration remains AVO-compliant. Velocity constraints, (e.g. well data, geobodies, gradients etc.) can be integrated into the imaging workflow as meshes for the tomography or as layers or bodies with predefined velocities.

References

Al-Chalabi, M. [2014]. *Principles of seismic velocities and time-to-depth conversion.* EAGE, Houten, The Netherlands.

Benson, C.E., Esestime, P. and Cvetkovic, M. [2015] Using Geological Constraints to Improve Velocity Model Building for Depth Imaging in Frontier Areas – Case Studies. *77th EAGE Conference and Exhibition,* Extended Abstracts.

Brownfield, M.E. [2016]. Assessment of Undiscovered Oil and Gas Resources of the Senegal Province, Northwest Africa. In: Brownfield, M.E (Ed.), *Geologic assessment of undiscovered hydrocarbon resources of Sub-Saharan Africa: U.S. Geological Survey Digital Serie 69-GG*, **2**, 2-20.

Davison, I. [2005]. Central Atlantic margin basins of North West Africa: Geology and hydrocarbon potential (Morocco to Guinea). *Journal of African Earth Sciences*, **43**, 254-274.

Esestime, P., Benson, C., Cvetkovic, M. and Spoors, S. [2016]. Reducing the gap between seismic imaging and geology: Horizon consistent velocity analysis and modelling for pre-stack time and depth migrations. *First Break,* **34**, 59-64.

Esestime, P., Cvetkovic, M., Rogers, J., Nicholls, H. and Rodriguez, K., [2018]. Combined pre-stack and post-stack interpretation for velocity model building and hydrocarbon prospectivity: a learning case study from 3D seismic data offshore Gabon. *First Break*, **36**, 99-103.

Guillaume, P., Montel, J.P., Hollingworth, S., Zhang, X., Prescott, A., Reinier, M., Jupp, R., Lambaré, G., Pape, O. and Cavalié, A. [2012]. Seismic imaging with multi-layer tomography. *First Break*, **30**, 85-90.

Sayers, B. and Cooke, R. [2018]. MSGBC: Where is the Next Success? *GeoExpro*, **15** (5), 20-23.

Soto, J.I., Flinch, J.F., Tari, G. [2017]. Permo-Triassic Basin and Tectonics in Europe, North Africa and the Atlantic Margins: A Synthesis. In: *Permo-Triassic Salt Provinces of Europe, North Africa and the Atlantic Margins,* **1**, 3-41.

Tiwari, D., Gao, W., Nangarla, A., Bhowmik, P. and Ben Sayers. [2020]. High Resolution Tomography in MSGBC Basin – Northwest Africa: a case study. *82nd EAGE Conference and Exhibition,* Extended Abstract.